

Origin of the symmetric dimers in the Si(100) surface

H. Shigekawa,^{*} K. Hata, K. Miyake, M. Ishida, and S. Ozawa

Institute of Materials Science, and Center for TARA, Tsukuba Advanced Research Alliance, University of Tsukuba, Tsukuba 305, Japan

(Received 2 January 1997; revised manuscript received 17 March 1997)

A phase defect consisting of a phase boundary in a dimer row was observed to exist and migrate in the symmetric dimer region of a Si(100) surface at about room temperature. When the phase defects migrate rapidly compared to the timescale of scanning tunneling microscopy (STM), it results in a symmetric image of dimers. In this case, since dimer flip-flop motion is limited to the domain boundaries of the dimer rows, most of the surface remains unchanged without the destruction of the $2\times$ anticorrelation of the buckled dimers along the dimer rows. Considering the obtained results and the fact that the electronic structures obtained by photoemission spectroscopy at room temperature agree well with the theoretical results calculated for a surface with asymmetric dimer structures, the symmetric dimer structure observed at room temperature is concluded to be caused by the characteristic properties of the phase defects. [S0163-1829(97)01924-3]

The geometric and electronic structures of the Si(100) surface have been studied extensively because of their importance, from both scientific and technological points of view. Top-layer atoms form dimers, which are imaged by scanning tunneling microscopy (STM) as a symmetric configuration at room temperature. However, it is widely accepted that dimers are buckled even at room temperature and switch back and forth between the two possible orientations very quickly compared to the time scale of STM measurement, which results in the observed symmetric configuration in the STM images.¹⁻⁷ In fact, the electronic structure of the Si(100) surface obtained by the photoemission spectroscopy at room temperature agrees with the theoretical results calculated for a surface with alternately buckled dimers.²

However, when the dimers flip-flop without correlation, the flip-flop motion implies a completely disordered surface, and the observed agreement in the electronic structure is not expected. To yield consistent agreement between the photoemission data and theoretical calculations, the $2\times$ anticorrelation of dimer buckling along a dimer row would have to persist up to $T\sim 300$ K. Such strongly anisotropic coupling between adjacent dimers was also predicted by the results of low-energy electron diffraction measurement.⁷ One possible mechanism to account for this is that the dimer switching occurs sequentially as a domain boundary, where two adjacent dimers are buckled in the same orientation.² When the phase defect at the boundary migrates rapidly compared to the time scale of STM, it results in the symmetric imaging of dimers in STM measurements. In this case, since dimer flip-flop motion is limited to the domain boundaries of the dimer rows, most of the surface remains in the $2\times$ anticorrelation along the dimer rows.

Although the idea explains the results well, the existence of such a defect was just an assumption. Recently, the existence of such a phase defect, called a type-*P* defect, was observed on a Si(100) surface by using STM at ~ 6 K.⁸ The type-*P* defect consists of two adjacent dimers that are buckled in the same orientation and was observed to migrate along a dimer row due to dimer flip-flop motion at the phase boundaries. Therefore, the symmetric dimer structure of the

Si(100) surface described above may be explained by the characteristic properties of the type-*P* defect.

In this paper, we present an analysis of the formation mechanism of the symmetric dimers in the Si(100) surface based on our STM results. A phosphorus-doped (~ 0.01 Ωcm) Si(100) sample surface was used. All images in this paper were taken in the constant-current mode.

Figure 1 shows an STM image taken at room temperature. The sample bias V_s and tunneling current were -2.0 V and 1.0 nA, respectively. Similarly to the previous room-temperature STM results, some dimers near defects are buckled; however, most dimers look symmetric. In order to clarify the structure of the symmetric dimer areas, we first examine the surface at ~ 6 K, where dimer flip-flop motion is almost frozen.

Figures 2(a) and 2(b) show STM images obtained continuously at ~ 6 K. Each area in both images shows the change taking place during a one-minute scan. Both $c(4\times 2)$ and $p(2\times 2)$ structures coexist, as previously reported.⁸ However, at some domain boundaries between the two phases, noisy flickering structures are seen. The $c(4\times 2)$, the $p(2\times 2)$, and the noisy flickering areas are colored green, blue, and gold, respectively.

At domain boundaries between the $c(4\times 2)$ (green) and $p(2\times 2)$ (blue) areas, one phase shifter, such as a type-*C* or a type-*P* defect, exists on a dimer row. From a comparison between the two images, some phase boundaries are seen to have moved, for example, from $A_1\sim C_1$ in Fig. 2(a) to $A_2\sim C_2$ in Fig. 2(b). Phase defects that have moved during the scan and the dimers of which the buckling angle changed according to the movement of the type-*P* defects are indicated by the red dots and open circles in Fig. 2, respectively. On the other hand, boundaries that did not move during the scan are indicated by \blacktriangledown in Fig. 2. Since type-*C* defects do not change their positions, while type-*P* defects do, the boundaries that did and did not move during a scan are formed by type-*P* and type-*C* defects, respectively. In fact, the phase defects indicated by \blacktriangledown show a brighter contrast than do other dimers, which is a characteristic property of the type-*C* defect.

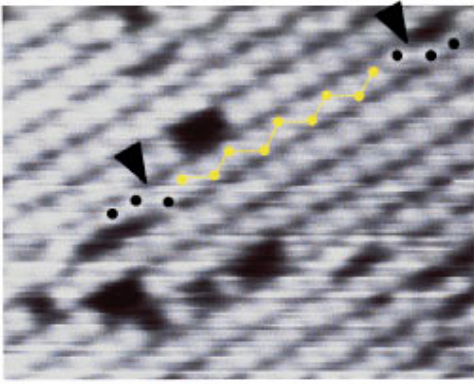


FIG. 1. (Color) STM image of Si(100) surface obtained at room temperature ($V_s = -2.0$ V, $I_s = 1.0$ nA). For a comparison, phase in the symmetric dimers on a row sandwiched between two fixed buckled dimer regions is indicated by yellow dots and bars.

At boundary A , five dimers changed their buckling angle to the opposite direction, and the type- P defect moved from A_1 to A_2 . In most areas, the dimer flip-flop motion was suppressed and the isolated motion of the type- P defect was observed similar to that at boundary A . However, some small domains with unstable dimers were observed as indi-

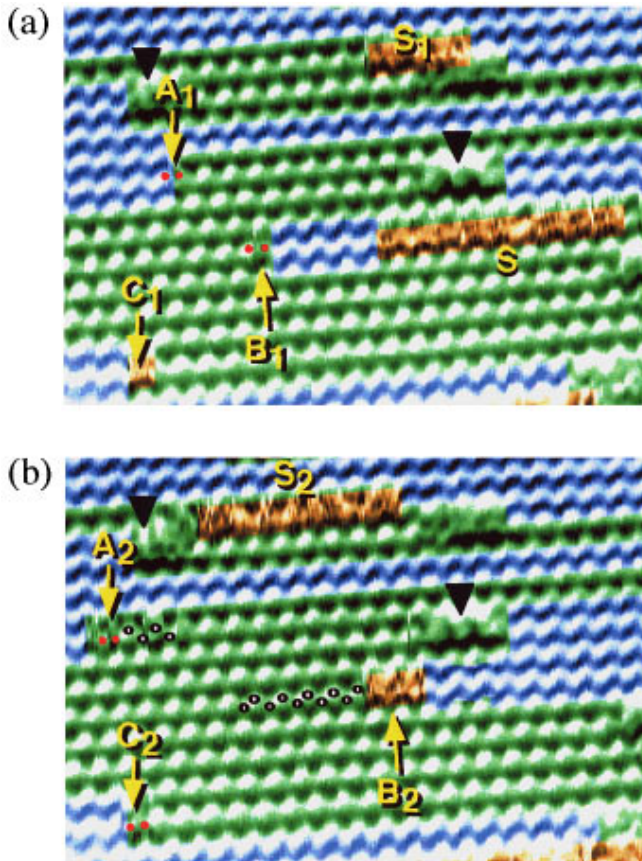


FIG. 2. (Color) STM images of Si(100) surface obtained continuously at ~ 6 K ($V_s = 1.5$ V, $I_s = 1.5$ nA). Each scan took 1 min. The $c(4 \times 2)$, the $p(2 \times 2)$, and the noisy flickering areas are colored green, blue, and gold, respectively. \blacktriangledown indicates type- C defects. The dimers of which the buckling angle changed during the scan are indicated by open circles in (b).

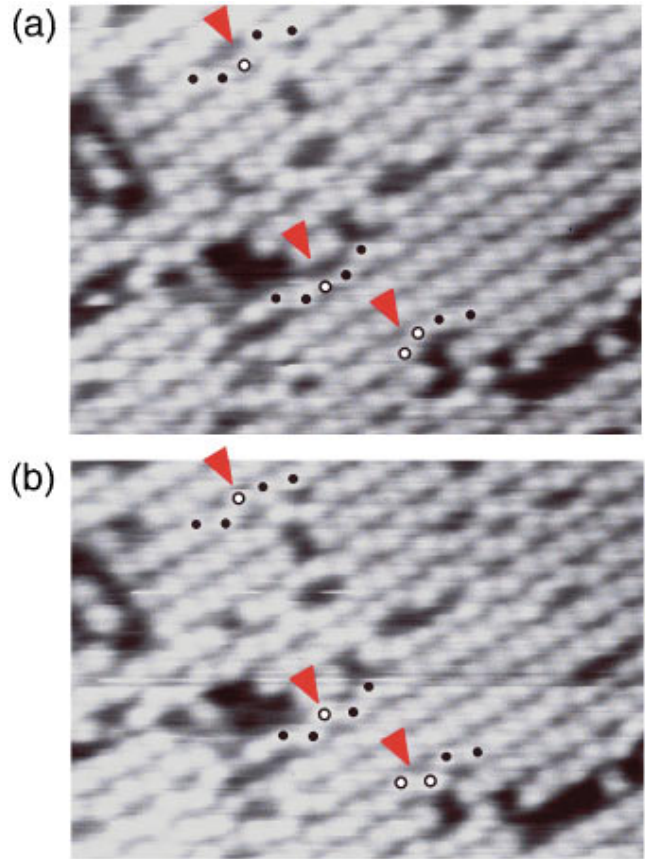


FIG. 3. (Color) (a), (b) Change in the structure of Si(100) surface during 1 min scan at room temperature ($V_s = -2.0$ V, $I_s = 1.0$ nA). The dimers of which the buckling angle changed during the scan are indicated by open circles in (b).

cated by gold areas in Fig. 2. Let us look at the relationship between the symmetric dimer structure and the type- P defect.

There was one type- P defect at the boundary B_1 , as indicated by red dots in Fig. 2(a). It moved to the right during a scan of about one minute and formed an unstable domain B_2 , as shown in Fig. 2(b). On the other hand, at boundary C_1 , only one dimer was unstable, as shown in Fig. 2(a), which stabilized and formed a phase defect C_2 , as shown in Fig. 2(b).

In general, at the noisy unstable dimer domains, C_1 , S_1 , and S in Fig. 2(a) and B_2 and S_2 in Fig. 2(b), the phase of the buckled dimers changes from one side to the other of the domains. Namely, these domains are sandwiched between rows of dimers that have $c(4 \times 2)$ (green) and $p(2 \times 2)$ (blue) arrangements with respect to their adjacent dimer rows. Therefore, at least one type- P defect exists in the unstable dimer areas.

As shown here, the dynamics of the dimer flip-flop motion caused by the type- P defect is related to the apparently symmetrical structure at 6 K. In this case, as described above, most of the surface area remains in the 2×1 anticorrelation structure along the dimer rows, which agrees with the experimental result obtained by photoemission spectroscopy. In order to elucidate the characteristics of the mechanism in more detail, we examine the dimer structures at room temperature.

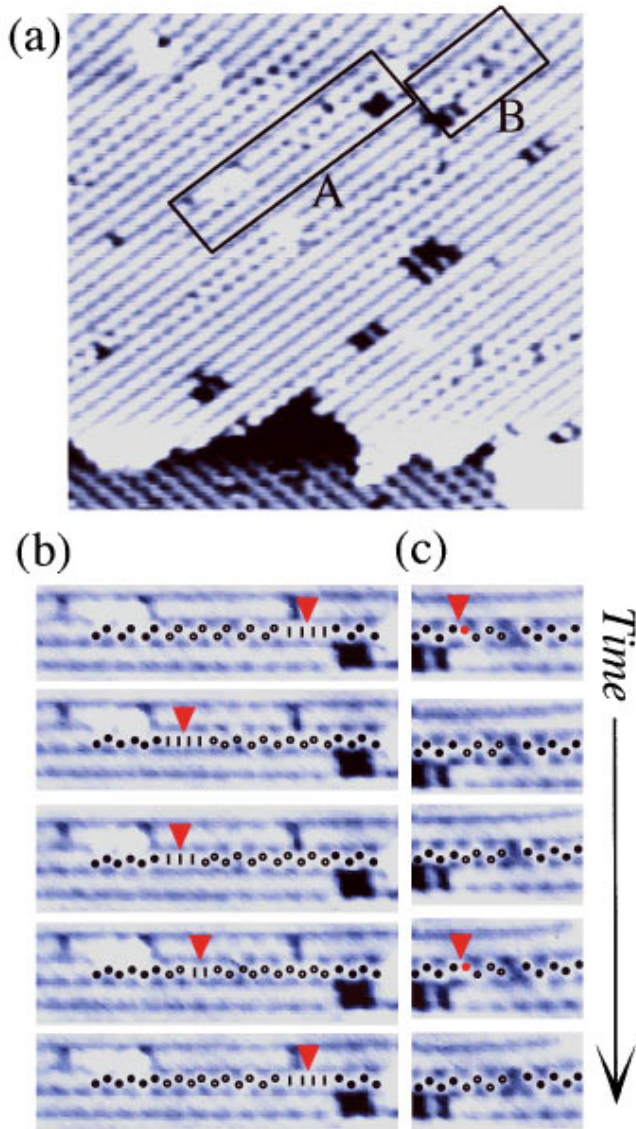


FIG. 4. (Color) (a) STM image of Si(100) surface obtained at ~ 200 K ($V_s = -2$ V, $I_s = 1.0$ nA). (b), (c) Magnifications of the areas indicated by squares A and B in (a), respectively. The five STM images in both (b) and (c) were obtained continuously. The time difference between each image is about 1 min. Fixed dimers, symmetric dimers, and the dimers that changed the buckling angle during the scans are indicated by solid circles, bars, and open circles, respectively.

Figures 3(a) and 3(b) show the STM images obtained for the same area in continuous scans at room temperature. Since it is difficult to analyze the structure of a completely symmetric dimer area, we show an area with a rather high atomic defect density here. By comparing Figs. 3(a) and 3(b), we see that the buckling angle of the dimers near the atomic defects indicated by the red arrows changed during scan that lasted about one minute, which may be related to the formation process of type-*P* defects. Here, stable dimer flip-flop motion was observed at room temperature because the motion is suppressed near the atomic defects.

Let us examine whether the type-*P* defect exists in the symmetric dimer regions, an example of which is shown in Fig. 1. Buckled dimers fixed by defects are indicated by solid

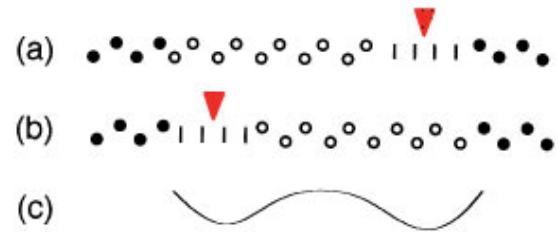


FIG. 5. (Color) (a), (b) Schematics of the typical structures in Fig. 4(b). (c) A potential model for the type-*P* defect in Fig. 4(b).

circles, and a yellow zigzag line is overlaid on the symmetric dimer region to help us compare the phases of the fixed buckled dimers indicated by the arrows at either end of the symmetric dimers. The phase of the fixed buckled dimers in the two regions is out of phase, and at least one type-*P* defect must exist in the symmetric dimer domain sandwiched between the two fixed buckled dimer regions. Therefore, the observed symmetric dimer structure along the dimer row in Fig. 1 is considered to be caused by the migration of the type-*P* defect, taking into account the results obtained at 6 K.

In order to study the characteristic properties of the type-*P* defect in the symmetric dimer region further, we observed the surface at a slightly lower temperature (~ 200 K). As is shown in Fig. 4(a) ($V_s = -2$ V, $I_s = 1.0$ nA), the buckled dimers extend further from the surface atomic defects than those at room temperature did, however, most of the dimers still remain symmetric at this temperature, similarly to the previous results.⁵

Figures 4(b) and 4(c) are magnifications of the areas indicated by squares A and B in Fig. 4(a). Acoustic noise from liquid nitrogen lowered the resolution, but the buckled dimers are clearly recognizable. In Fig. 4(b), a symmetric dimer region exists on a dimer row sandwiched between two buckled dimer regions, similarly to that in Fig. 1. Fixed dimers, symmetric dimers, and the dimers that changed the buckling angle during the scans are indicated by solid circles, bars, and open circles, respectively. By comparing the phase of the buckled dimers on either side of the symmetric dimer area, we see that there is one type-*P* defect in the symmetric dimer region, similarly to the case in Fig. 1. However, since the temperature is lower and the dimer flip-flop motion is more suppressed in this case, the symmetric dimers are limited to a smaller area, as expected. As is shown in Fig. 4(b), the symmetric dimer area changed its position with time due to the migration of the included type-*P* defect. The observed results agree well with the mechanism described above; the symmetric dimers are caused by the migration of the phase defects of dimer rows.

As is shown in Fig. 4(b), the symmetric dimer region changes its position according to the migration of the type-*P* defect, but is located only around the sides of the dimer domain and never appears in the central part. Figures 5(a) and 5(b) show the schematics of two typical STM images. The observed results suggest the potential shape shown in Fig. 5(c) for the type-*P* defect, as a function of its position along the dimer row. The observed result may be related to the tendency for the $2x$ ordering of the dimer arrangement along a dimer row, however, in order to clarify the detailed mechanism, further experiment is necessary.

Finally, let us investigate how the type-*P* defects can be

introduced. Figure 4(c) shows an STM image near a type-A defect, i.e., a vacancy of a dimer.³ In the first image, there is one type-*P* defect on the left side of the type-A defect as indicated by an arrow. In consideration of the buckling angle of the dimers, the type-*P* defect disappeared through the type-A defect in the second image. As shown in the following STM images, another type-*P* defect is introduced in the fourth image, but it disappears again in the fifth image. This is one of the possible mechanisms by which type-*P* defects are introduced into the surface. At room temperature, similar process is seen in Fig. 3, and creation and annihilation of the type-*P* defects are also expected.⁸

In conclusion, a phase defect of dimer rows was observed to exist and migrate in the symmetric dimer regions of the Si(100) surface at around room temperature. When the phase defects migrate rapidly compared to the time scale of STM

measurement, symmetric dimers can be formed without completely destroying the $2\times$ anticorrelation arrangement, which agrees well with the fact that the electronic structure obtained by photoemission spectroscopy at room temperature is consistent with the theoretical result calculated under the assumption of ordered asymmetric dimers. Considering these results, the symmetric dimers in the Si(100) surface are concluded to be caused by the characteristic properties of the type-*P* phase defect of the dimer rows.

This work was supported by the Shigekawa Project of TARA, University of Tsukuba. The support of a Grant-in-Aid for Scientific Research from the Ministry of Education, Science, and Culture of Japan is also acknowledged. One of the authors (K.M.) would like to thank Japan Society for the Promotion of Science (JSPS) for financial support.

*Corresponding author.

Electronic address: hidemi@mat.ims.tsukuba.ac.jp
<http://www.ims.tsukuba.ac.jp/lab/shigekawa/index.html>

¹R. Tromp, R. Hamers, and J. Demuth, Phys. Rev. Lett. **59**, 2071 (1987).

²J. E. Northrup, Phys. Rev. B **47**, 10 032 (1993).

³R. Hamers, R. Tromp, and J. Demuth, Phys. Rev. B **34**, 5343 (1986).

⁴R. Wolkow, Phys. Rev. Lett. **68**, 2636 (1992).

⁵A. Smith, F. Men, K. Chao, and C. Shih, J. Vac. Sci. Technol. B **14**, 914 (1996).

⁶A. W. Muntz, Ch. Ziegler, and W. Gopel, Phys. Rev. Lett. **74**, 2244 (1995).

⁷M. Kubota and Y. Murata, Phys. Rev. B **49**, 4810 (1994).

⁸H. Shigekawa *et al.*, Jpn. J. Appl. Phys. **35**, L1081 (1996); **36**, L294 (1997).